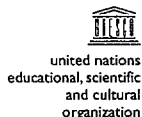


the



**abdus salam**  
international  
centre  
for theoretical  
physics

IC/2000/78



XA0100994

**MACROSCOPIC ANGULAR-MOMENTUM  
STATES OF BOSE-EINSTEIN CONDENSATES  
IN TOROIDAL TRAPS**

**M. Benakli**

**S. Raghavan**

**A. Smerzi**

**S. Fantoni**

**and**

**S.R. Shenoy**

32 / 21

preprint

INTERNATIONAL ATOMIC ENERGY AGENCY



INIS Section

**INFORMATION NOTE**

Dear User,

The title of this document has erroneously entered the INIS Database as:  
**'Macroscopic angular-momentum stages of Bose-Einstein condensates in toroidal traps'**.

The correct full title is: **'Macroscopic angular-momentum states of Bose-Einstein condensates in toroidal traps'**.

We will rectify this error in the INIS Database accordingly.

We apologize for the inconvenience this has caused.

Inquiries should be mailed to:

International Atomic Energy Agency  
INIS Section  
P. O. Box 100  
Wagramerstrasse 5  
A-1400 Vienna  
Austria

Fax: (+43) 1 26007 or (+43) 1 2600 29882  
Phone: (+43) 1 2600 ext. 22866, 22869 or 22870  
E-mail: [chouse@iaea.org](mailto:chouse@iaea.org)

United Nations Educational Scientific and Cultural Organization  
and  
International Atomic Energy Agency

THE ABDUS SALAM INTERNATIONAL CENTRE FOR THEORETICAL PHYSICS

**MACROSCOPIC ANGULAR-MOMENTUM STATES OF  
BOSE-EINSTEIN CONDENSATES IN TOROIDAL TRAPS**

M. Benakli, S. Raghavan

*The Abdus Salam International Centre for Theoretical Physics, Trieste, Italy,*

A. Smerzi

*International School for Advanced Studies, Trieste, Italy*

*and*

*Istituto Nazionale di Fisica della Materia, Trieste, Italy,*

S. Fantoni

*International School for Advanced Studies, Trieste, Italy,*

*Istituto Nazionale di Fisica della Materia, Trieste, Italy*

*and*

*The Abdus Salam International Centre for Theoretical Physics, Trieste, Italy*

*and*

S.R. Shenoy

*The Abdus Salam International Centre for Theoretical Physics, Trieste, Italy.*

MIRAMARE – TRIESTE

March 2001

**Abstract.** – We study the stability of a rotating repulsive-atom Bose-Einstein condensate in a toroidal trap. The resulting macroscopic angular-momentum states with integer vorticity  $l$  spread radially, lowering rotational energies. These states are robust against vorticity-lowering decays, with estimated metastability barriers capable of sustaining large angular momenta ( $l \lesssim 10$ ) for typical parameters. We identify the centrifugally squashed  $l$ -dependent density profile as a possible signature of condensate rotation and superfluidity.

Bose-Einstein condensates (BEC) of atoms in magnetic/optical traps have been the focus of intense recent activity [1-12]. The macroscopic phase-coherence of the BEC wave function was demonstrated by the observation of interference fringes in the overlap region of two freely spreading condensates [2], after the confining traps were switched off. However, the superfluid character of the interacting BEC is most clearly tested through the sustainability of supercurrents. Non-destructive tests of phase-coherence and superfluidity, through Josephson-like effects have been proposed [6-9], including novel self-trapping phenomena and  $\pi$ -mode oscillations [7,8]. A direct test of superfluidity in bulk superfluids/superconductors is the observation of quantized vortices [13,14] maintained by superflows. In multiply connected geometries (*e.g.*, thick superconducting cylinders [15] or superfluids in narrow rings), metastable superflows with azimuthally symmetric wave functions [16-18] maintain rotational states having integer vorticity  $l$ . Such states have been considered [17,18] in the uniform-density limit, with the BEC rigidly restricted to flat-potential regions by (narrow-ring) rigid walls. But one must go beyond this “square-well container” limit, to capture the number-dependent spread of repulsive BEC atoms in a polynomial trap. Vortices centered in (simply connected) harmonic traps have been found by solving the Gross-Pitaevskii equation (GPE) [10,11], and in dynamic vortex nucleation studies [19]. However, such vortices could be unstable to outward displacements [12].

Consequently, to test for the superfluidity of BEC, it is imperative to investigate *non-uniform rotating metastable* states, in *multiply connected* toroidal traps.

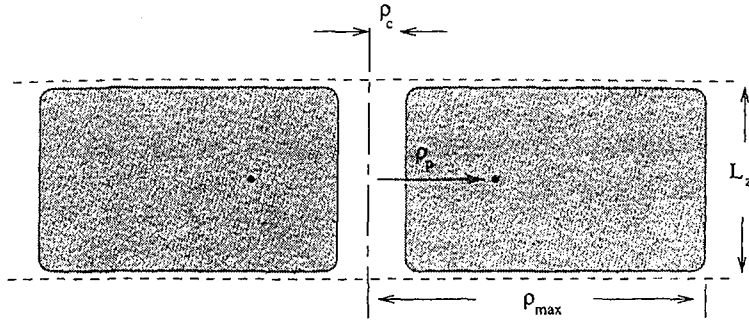


Fig. 1. – Schematic plot of quasi-2D “doughnut” toroid geometry with laser along the  $z$ -axis. The trap potential rises sharply (dashed boundary) at  $|z| = L_z/2$ . Here  $\rho_c$ ,  $\rho_p$ , and  $\rho_{\max}$  are the effective core radius, toroidal axis, and extent of the (shaded) BEC cloud, respectively.

In this letter we consider  $N$  condensate atoms at zero temperature, in an elliptical trap, with an axial “hole” (or strong potential barrier) drilled by an intense off-resonant laser beam, forming an effective 2D toroidal trap. We demonstrate the existence of  $l \neq 0$  rotational states, and examine related issues such as: i) the mixing of different  $l$ -states due to the nonlinear interaction in the GPE; ii) the effects of off-center displacements of the toroidal hole; iii) the existence of metastability barriers, and of decay channels limiting the accessible  $l$ -values. A central result is that the interaction-induced outward spread of the wave function reduces the  $l$ -state rotational energies, permitting relatively large  $l$ -values to be sustained by metastability barriers. Three possible activated decay mechanisms are found to have similar characteristic barriers: vorticity can boil off in all three lowest channels simultaneously, for  $l > l_{\max} \sim N^{1/4}$ .

i) *GPE and  $l$ -states*: The macroscopic condensate wave function  $\Psi(\rho, \theta, z) = \sqrt{N} \Phi(\rho, \theta, z)$  obeys the GPE, that in cylindrical coordinates reads

$$\left[ -\frac{\hbar^2}{2m} \left( \frac{\partial^2}{\partial \rho^2} + \frac{1}{\rho} \frac{\partial}{\partial \rho} + \frac{1}{\rho^2} \frac{\partial^2}{\partial \theta^2} + \frac{\partial^2}{\partial z^2} \right) + V_{\text{trap}}(\rho, \theta) + V_{\text{trap}}(z) + U_0 |\Psi|^2 \right] \Psi = \mu \Psi, \quad (1)$$

where  $U_0 = 4\pi\hbar^2 a/m$ ,  $a$  is the  $s$ -wave scattering length (taken to be positive  $a > 0$ ), and  $\mu$  is the chemical potential.  $V_{\text{trap}}(z)$  is harmonic with a curvature  $\omega_z$  up to  $|z| \sim L_z/2$ , beyond which it rises sharply, as in fig. 1, dashed line.  $V_{\text{trap}}(\rho, \theta)$  is formed from the combination of a harmonic potential, and a far-off-resonant Gaussian-profile laser barrier of high intensity  $V_c$  and width  $2\sigma$ , giving an axially symmetric “doughnut” trap:

$$V_{\text{trap}}(\rho, \theta) \rightarrow V_{\text{trap}}(\rho) = \frac{1}{2} m \omega_{\parallel}^2 \rho^2 + V_c e^{-\rho^2/2\sigma^2}. \quad (2)$$

The interacting BEC cloud is blocked from expanding beyond  $|z| \lesssim L_z/2$ , spreading only radially with increasing  $N$ . Then the BEC wave function is quasi-2D, *i.e.*, uniform  $\sim 1/\sqrt{L_z}$  in the  $z$ -direction, so that

$$\Phi_l(\rho, \theta, z) \rightarrow \Phi_l(\rho, \theta) = \frac{\bar{\Phi}_l(\bar{\rho})}{\sqrt{L_z r_{\parallel}}} \frac{e^{il\theta}}{\sqrt{2\pi}}, \quad (3)$$

where  $l$  is integer. We scale lengths (energies) in the harmonic trap length  $r_{\parallel} \equiv (\hbar/m\omega_{\parallel})^{1/2}$  (zero-point energy =  $\hbar\omega_{\parallel}/2$ ), so  $\bar{\rho} \equiv \rho/r_{\parallel}$ ,  $\bar{\sigma} \equiv \sigma/r_{\parallel}$ ,  $\bar{\mu}_l \equiv \mu_l/\frac{1}{2}\hbar\omega_{\parallel}$ , and  $\bar{V}_c \equiv V_c/\frac{1}{2}\hbar\omega_{\parallel}$ . Then

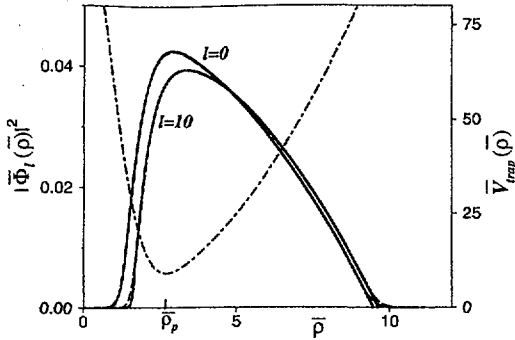


Fig. 2

Fig. 2. – Trap potential (right vertical axis, dash-dotted line)  $\bar{V}_{\text{trap}}(\bar{\rho})$  vs. cylindrical-coordinate radius,  $\bar{\rho}$ , (with bars denoting scaling in harmonic trap energy/length).  $\bar{\rho}_p$  is the effective toroidal trap minimum. Scaled BEC density  $|\bar{\Phi}_l(\bar{\rho})|^2$  (left vertical axis) vs.  $\bar{\rho}$  from analytic (solid line) and numerical (dashed line) results. Parameters are as in text.

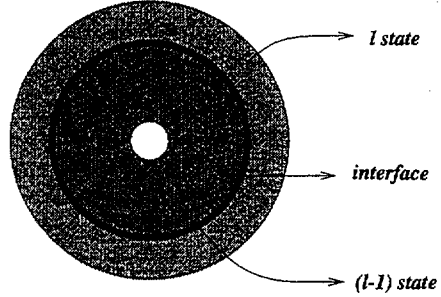


Fig. 3

Fig. 3. – Schematic of a superposition of  $l, (l-1)$  vortex states overlapping at an interface of thickness  $\sim 2\xi$ .

eq. (1), in dimensionless form, is

$$\left[ - \left( \frac{d^2}{d\bar{\rho}^2} + \frac{1}{\bar{\rho}} \frac{d}{d\bar{\rho}} \right) + \frac{l^2}{\bar{\rho}^2} + \bar{V}_{\text{trap}}(\bar{\rho}) + \bar{N} |\bar{\Phi}_l(\bar{\rho})|^2 \right] \bar{\Phi}_l(\bar{\rho}) = \bar{\mu}_l \bar{\Phi}_l(\bar{\rho}), \quad (4)$$

with  $\bar{N}$  defining a dimensionless expansion parameter,

$$\delta \equiv \bar{N}^{-1/2} \equiv \frac{1}{2} \left( \frac{L_z}{aN} \right)^{1/2}. \quad (5)$$

As shown in fig. 2, the toroidal trap potential has a minimum around the toroidal axis at  $\rho = \rho_p$ , where  $\rho_p = \sqrt{2}\sigma[\ln \bar{V}_c/2\bar{\sigma}^2]^{1/2}$ . A non-interacting BEC in such a minimum has an approximately Gaussian shape with a 2D “volume”  $\sim r_{\parallel}^2$ . However, the interacting BEC spreads (as seen later) to  $\rho_{\text{max}} \propto N^{1/4}, \gg r_{\parallel}$ . The parameter  $\bar{N}^{-1/2}$  of eq. (5) is then essentially the volume ratio of the non-interacting and interacting BEC, viz.  $\delta \sim r_{\parallel}^2/\rho_{\text{max}}^2, \ll 1$  for large  $N$ . This is the small expansion parameter in the problem.

We have solved eq. (4) numerically. However in the regime  $\delta \ll 1$ , and for a sufficiently low-width laser-hole,  $\bar{\sigma} \ll \delta^{-2/13}$ , we can drop the derivatives  $\sim \delta$  in eq. (4) and analytically calculate the wave function in the Thomas-Fermi approximation (TFA) [3-5]

$$\bar{\Phi}_l(\bar{\rho}) = \left( \frac{\bar{\mu}_0}{\bar{N}} \right)^{1/2} \left[ 1 + \{ \bar{\mathcal{E}}_l - l^2/\bar{\rho}^2 - \bar{V}_{\text{trap}}(\bar{\rho}) \} / \bar{\mu}_0 \right]^{1/2}, \quad (6)$$

where  $\bar{\mathcal{E}}_l \equiv \bar{\mu}_l - \bar{\mu}_0$  is the difference between the  $l \neq 0$  and  $l = 0$  chemical potentials. The TFA wave function drop to zero at two points  $\bar{\Phi}_l(\bar{\rho}_{\text{max}}) = \bar{\Phi}_l(\bar{\rho}_{\text{min}}) = 0$ .

To describe the wave function near the center, where derivatives contribute, we have matched the TFA wave function to a polynomial (up to  $\rho^{l+4}$ ) solution  $\bar{\Phi}_l^<$  inside an effective “core”  $\bar{\rho}_c \gtrsim \bar{\rho}_{\text{min}}$ .

The chemical potentials are determined by normalization condition:

$$\int_{\bar{\rho}_c}^{\bar{\rho}_{\max}} d\bar{\rho} |\bar{\Phi}_l(\bar{\rho})|^2 + \int_0^{\bar{\rho}_c} d\bar{\rho} |\bar{\Phi}_l^<(\bar{\rho})|^2 = 1. \quad (7)$$

With the first integral dominating, we have

$$\bar{\mu}_l \simeq 2\bar{N}^{1/2} + \lambda l^2 \bar{N}^{-1/2}. \quad (8)$$

In eq. (8),  $\lambda \equiv \ln(\bar{\rho}_{\max}/\bar{\rho}_c)$ , where  $\bar{\rho}_c \sim \bar{\sigma}[\ln(\bar{V}_c/\bar{\mu}_0)]^{1/2}$ , so the results are only very weakly dependent ( $\lambda \sim \ln \bar{\rho}_c$ ) on the toroidal core region and how it is modeled. The interaction indeed pushes the BEC of eq. (6). Far beyond the toroidal axis, and with  $\bar{\rho}_m \equiv \bar{\rho}_{\max}(l=0) = (4\bar{N})^{1/4}$ , we have

$$\bar{\rho}_{\max}(l) \simeq \bar{\rho}_m(1 + (\lambda - 1/2)l^2/4\bar{N}). \quad (9)$$

Centrifugal energy contributions in eq. (8) ( $\bar{E}_l \propto l^2/\bar{\rho}_m^2 \sim l^2/\bar{N}^{1/2}$ ) are lowered due to this interaction-driven spread, so larger  $l$ -values are sustainable by given metastability barriers.

The local density difference due to centrifugal effects is

$$|\bar{\Phi}_l(\bar{\rho})|^2 - |\bar{\Phi}_{l=0}(\bar{\rho})|^2 \simeq \lambda l^2 \bar{N}^{-3/2} [1 - (\bar{\rho}_m^2/2\lambda\bar{\rho}^2)], \quad (10)$$

with  $\bar{\Phi}_l(\bar{\rho})$  peaking at  $\bar{\rho} = \bar{\rho}_{\text{peak}} \approx \bar{\rho}_p + (2\bar{\sigma}^2/\bar{\rho}_p^4)l^2$ . Figure 2 shows  $|\bar{\Phi}_l(\bar{\rho})|^2$  vs.  $\bar{\rho}$ , for  $l = 0$  and 10, for parameters as given later. The analytic approximation (solid line) closely matches the (dashed line) numerical solution of eq. (4). The centrifugal reduction ( $\sim 10\%$  for  $l = 10$ ), with outward shift, of the density peak, is a rotation signature, possibly detectable by phase contrast imaging [20]. The super-current density is  $j \sim \hbar/(im\bar{\rho})\Psi^* \frac{\partial}{\partial \theta} \Psi = N|\bar{\Phi}_l(\bar{\rho})|^2 v_{s\theta}$ , where the azimuthal velocity  $v_{s\theta} = (\hbar l/m\rho)$ , and  $j$  vanishes at the origin as  $j \sim \rho^{2l+3}$ . The laser hole ‘‘pins’’ the azimuthal velocity of average angular momentum  $\langle \Psi_l | (\hbar/i)\partial/\partial\theta | \Psi_l \rangle = Nl\hbar$ , suppressing displacement instabilities [12, 18]. We stress here that since our configuration uses a physically reasonable Gaussian-profile toroidal laser barrier (instead of an infinite core), the wave functions are smooth, and vanish only at the origin. Consequently the energies remain positive in the entire region and instability-generating negative energy core states [10, 12] do not arise.

In practice, the toroidal ‘‘hole’’ of fig. 1 could be drilled off the trap axis, or the laser could fluctuate in profile and position. With such a relative displacement  $\vec{\rho} = (\rho_0, \theta)$  of the trap is  $V_{\text{trap}}(\rho) \rightarrow V_{\text{trap}} + \bar{\rho}_0^2 - 2\bar{\rho}_0\bar{\rho}\cos\theta$ , modifying the TFA solution of eq. (6). The BEC cloud becomes anisotropic, extending to  $\bar{\rho}_m = \bar{\rho}_0 \cos\theta + \bar{\mu}_0^{1/2}$ . However, global averages of the energy/angular momentum and barrier heights are unaffected, to order  $\sim \bar{\rho}_0/\bar{\rho}_m \sim \bar{N}^{-1/4} \ll 1$ .

ii) *Metastability barriers to direct  $l \rightarrow (l-1)$  transitions:* We first consider  $l$  states jumping uniformly into  $l-1$  states. The non-linear term in the GPE disfavors the overlap of  $l$ -states and induces barriers against direct  $l \rightarrow (l-1)$ -decays: interatomic collisions disfavor the transition-state slowing-down of a minority fraction ( $< 1/2$ ) of the rotating flow. A GPE trial function for full superposition is  $\bar{\Phi}(\bar{\rho}, \theta) = [C_l \bar{\Phi}_l(\bar{\rho}, \theta) + C_{l-1} \bar{\Phi}_{l-1}(\bar{\rho}, \theta)]$ , with variational constants,  $|C_l|^2 + |C_{l-1}|^2 = 1$ . The free energy functional  $\bar{F}(\bar{\Phi})$  is then

$$\frac{\bar{F}}{\bar{N}} = \sum_{p=l, l-1} (|C_p|^2 - 2)|C_p|^2 I_{p,p} + 4|C_l|^2 |C_{l-1}|^2 I_{l, l-1}, \quad (11)$$

where  $I_{l, l'} \equiv \frac{1}{2}\bar{N} \int_0^\infty d\bar{\rho} |\bar{\Phi}_l(\bar{\rho})|^2 |\bar{\Phi}_{l'}(\bar{\rho})|^2$  is the overlap integral. The  $l$ -state  $(C_l, C_{l-1}) = (1, 0)$  is separated from the  $(l-1)$ -state  $(0, 1)$  by a transition state  $(1/2, 1/2)$ . This ‘‘full-overlap’’

$\bar{F}/N$  barrier relative to the (1,0) state is  $\bar{\mathcal{E}}_{B0} \approx \bar{\mu}_0/2 \sim \bar{N}^{1/2}$ , and larger than the splitting,  $\Delta\bar{\mathcal{E}}_l \equiv \bar{\mathcal{E}}_l - \bar{\mathcal{E}}_{l-1} = (2l-1)\lambda/\sqrt{\bar{N}}$ . The  $l$ -state is preserved by metastability barriers for  $\bar{\mathcal{E}}_l = l^2\lambda/\sqrt{\bar{N}} < \bar{\mathcal{E}}_{B0}$  up to a maximum value  $l < l_{\max 0} \sim \bar{N}^{1/2}$ .

Lower barriers are expected, for the (more physical) nucleation of “critical droplets”. Figure 3 shows such non-uniform  $l$ -states normalized in fractional volumes  $\nu_l, \nu_{l-1}$ . These overlap only at an interface of thickness  $2\xi$  and overlap fraction  $f \equiv (\nu_l + \nu_{l-1} - 1) > 0$ , thus reducing the  $l, (l-1)$  interspecies scattering [21]. We take  $\bar{\Phi}_p(\rho) \rightarrow \bar{\Phi}_p(\bar{\rho})g_p(\bar{\rho})$  where the step-function  $g_{l-1}(\bar{\rho})$  ( $g_l(\bar{\rho})$ ) is unity for  $\nu_{l-1}\bar{\rho}_m^2 > \bar{\rho}^2 > \bar{\rho}_c^2$  (for  $\bar{\rho}_m^2 > \bar{\rho}^2 > (1-\nu_l)\bar{\rho}_m^2$ ) and zero otherwise. Repeating the previous argument with these wave functions, we find that confinement to a reduced volume,  $\nu_p\bar{\rho}_m^2 < \bar{\rho}_m^2$ , increases the intra-species scattering:  $I_{pp}(\nu_p) = I_{pp}(\nu=1)/\nu_p$ . The (reduced) inter-species scattering gives  $I_{l,l-1}(\nu_l) \simeq (f/\nu_l\nu_{l-1})I_{l,l-1}(\nu=1)$ . The lowest interface-overlap barrier  $\bar{\mathcal{E}}_{B1}$ , or “critical droplet” energy, is obtained for approximately equal volume fractions  $\nu_l = \nu_{l-1} \gtrsim 1/2$ , giving an annular overlap volume of radius  $\bar{\rho}_m/\sqrt{2}$  and thickness  $\sim 2\xi$ , so the fractional overlap is then  $f = 2\sqrt{2}\xi/\bar{\rho}_m$ .  $\bar{\mathcal{E}}_{B1}$  is this fraction of the full-overlap barrier,  $\bar{\mathcal{E}}_{B1} \sim 2\sqrt{2}(\xi/\bar{\rho}_m)\bar{\mathcal{E}}_{B0}$  (gradient contributions omitted in TFA would be comparable). Here  $\bar{\xi} \sim 1/[\bar{N}|\bar{\Phi}_l(\bar{\rho}_p)|^2]^{1/2} \sim 1/\bar{\mu}_0^{1/2}$  is a “healing length”, so (scaled) barriers are of order of unity,  $\bar{\mathcal{E}}_{B1} = \sqrt{2} \sim O(1) \ll \bar{\mathcal{E}}_{B0}$ . The  $l$ -states are “robust” against decays for  $\mathcal{E}_B/\mathcal{E}_l \gtrsim 1$ , i.e., for  $l \lesssim l_{\max 1} = (\sqrt{2}/\lambda)^{1/2}\bar{N}^{1/4}$ . Note that it is the interaction-induced lowering of  $\bar{\mathcal{E}}_l$  that enables allows  $l_{\max}$  to be large. The estimates hold also for other “droplet” geometries: wedge-shaped regions of  $(l-1)$  states, expanding azimuthally, would have  $\sim (2\xi/\bar{\rho}_m)\bar{\mathcal{E}}_{B0}$  interface costs, and similar  $l_{\max 1} \sim \bar{N}^{1/4}$  scaling.

An external angular velocity,  $\Omega \equiv \bar{\Omega}(\frac{1}{2}\omega_{\parallel})$ , produced by an imposed rotation will cause an  $l=1$  to  $l=0$  transition, only above critical values,  $|\bar{\Omega}| \geq \bar{\Omega}_{cl} = \bar{\mathcal{E}}_{B1}$ . This estimate exceeds an  $\bar{\Omega}_{cl} \sim |\Delta\bar{\mathcal{E}}_l|$  estimate [4] based on the splitting alone.

iii) *Metastability barriers to mediated  $l \rightarrow (l-1)$  transitions:* An  $l$ -state could also decay, mediated by excitations. Nucleation of (rectangular) unit-vortex loops, with straight segments of vorticity  $J_z = -1$  would reduce core vorticity by  $l \rightarrow (l-1)$ . This core repels the  $J_z = 1$  loop-segment outwards by an interaction  $\sim -(l-1)\ln\rho$  [22]. (As  $v_{s\theta}\bar{\rho} \sim hl/m$  is a constant, there is no additional loop-expanding current-drive force [14].) The atomic density near the core is  $|\bar{\Phi}(\bar{\rho}_c)|^2 \sim \bar{\sigma}$  (independent of  $\bar{N}$ ), yielding a vortex-segment nucleation cost of  $\bar{\mathcal{E}}_{B2} \sim \bar{\xi}^2\bar{N}|\bar{\Phi}_l(\bar{\rho}_c)|^2 \sim \bar{\sigma}$ . For metastability,  $\bar{\mathcal{E}}_l = \lambda l^2/\sqrt{\bar{N}} < \bar{\mathcal{E}}_{B2}$  and the states are robust up to  $l \leq l_{\max 2} \sim \sqrt{\bar{\sigma}}\bar{N}^{1/4}/\sqrt{\lambda}$ .

Finally, another possible mediated-decay channel is a successive reduction  $N \rightarrow N-2$  of BEC  $l$ -state atoms, producing surface pairs of dissipative quasiparticles [11] of Bogoliubov excitation energy  $2\bar{\Delta}$ , and total angular momentum  $2l$  [17,18], that damps to zero. A detailed analysis [16] for toroidal traps is beyond the scope of this paper; however, for  $\bar{\mathcal{E}}_l \lesssim \bar{\Delta}$ , the quasiparticle channel is not accessed for  $l \lesssim l_{\max 3} = \sqrt{\bar{\Delta}}\bar{N}^{1/4}$ . (In other contexts [23], damping due to quasiparticles [10,12] is small.) Thus we find that  $l$ -states are robust to droplet/vortex-loop/quasiparticle decay channels, up to maximum values all scaling in the same way,  $\sim \bar{N}^{1/4}$ . Since the channels are activated over free-energy barriers  $N\bar{\mathcal{E}}_B$ , low temperatures exponentially favour rotational stability.

iv) *Numerical estimates:* Parameters chosen are  $\omega_{\parallel} = 132 \text{ rad s}^{-1} \sim 1 \text{ nK}$ ,  $\tau_{\parallel} = 4.6 \mu\text{m}$ ,  $L_z = 25 \mu\text{m}$ ,  $2\sigma = 12 \mu\text{m}$ ,  $a = 50 \text{ \AA}$ ,  $V_c = 63 \text{ nK}$ , and  $m = 3.84 \times 10^{-26} \text{ kg}$  (sodium). Then  $\rho_p = 18.4 \mu\text{m}$ , and for  $N = 10^6$ , we have  $\delta = 1/\sqrt{\bar{N}} = 0.03$ . Physical magnitudes are then  $\mu_0 = 32 \text{ nK}$ ,  $\lambda = 2$ ,  $\mathcal{E}_l = 0.031l^2 \text{ nK}$ ,  $\rho_m = 50 \mu\text{m}$ ,  $\xi = 0.8 \mu\text{m}$ ,  $v_{s\theta}(\rho) \leq v_{s\theta}(\rho_c) = 0.1l \text{ mm s}^{-1}$ ,  $\Omega_{cl} = 30 \text{ Hz}$ , yielding, for example,  $l_{\max 1} \sim 10$ .



Finally, we present a  $\bar{N}$ -scaling argument, extending our results to a general anharmonic  $d$ -dimensional toroidal trap. Consider a trap potential that, for distances  $\bar{r}$  well away from the toroidal core, is  $V_{\text{trap}} \sim \hbar\omega_t \bar{r}^\alpha$ , where  $\bar{r} \equiv r/r_t$  and  $r_t \equiv (\hbar/m\omega_t)^{1/2}$ . For  $\alpha = 2$  the trap is harmonic; for  $\alpha \rightarrow \infty$ , a square-well container results. We define  $\bar{N} \equiv (NU_0/\hbar\omega_t r_t^d)$ ,  $\bar{\Phi}(\bar{r}) \equiv \Phi(r)r_t^{d/2}$ ,  $\bar{\mu}_l \equiv \mu_l/\hbar\omega_t$ . The TFA wave function,  $\bar{\Phi}_l$  is almost flat,  $|\bar{\Phi}_l(\bar{r})| \simeq |\bar{\Phi}_0| \approx (\bar{\mu}_0/\bar{N})^{1/2}$ , and the BEC spreads until  $\bar{r} \simeq \bar{r}_m$ , when the confining potential rises to the chemical potential,  $\bar{\mu}_l \sim \bar{r}_m^\alpha$ . With the normalization integral  $\simeq |\bar{\Phi}_0|^2 \bar{r}_m^d = 1$ , we obtain  $\bar{r}_m = \bar{N}^{1/(\alpha+d)}$ . Then the  $l \neq 0$  excitation energies are  $\bar{\mathcal{E}}_l \sim l^2/\bar{r}_m^2$ , and the healing length is  $\bar{\xi} \sim (\bar{N}|\bar{\Phi}_0|^2)^{-1/2} \sim \bar{N}^{-\alpha/2(\alpha+d)}$ . We estimate the metastability barriers to decays via full-overlaps, interfaces, and nucleated vortices to be  $\bar{\mathcal{E}}_{B0} \sim \bar{N}^{\alpha/(\alpha+d)}$ ,  $\bar{\mathcal{E}}_{B1} \sim \bar{N}^{(\alpha-2)/2(\alpha+d)}$ , and  $\bar{\mathcal{E}}_{B2} \sim \bar{N}^{(d-2)/(\alpha+d)}$ , respectively. (Since  $\bar{N} \sim NU_0$ , the barriers vanish in the ideal-gas limit,  $U_0 \rightarrow 0$ .) The corresponding robustness bounds are  $l_{\text{max}0} \sim \bar{N}^{(2+\alpha)/2(\alpha+d)}$ ,  $l_{\text{max}1} \sim \bar{N}^{(2+\alpha)/4(\alpha+d)}$ ,  $l_{\text{max}2} \sim \bar{N}^{d/2(\alpha+d)}$ , respectively. For the  $\alpha = 2$  harmonic trap in 2D, we recover our results:  $l_{\text{max}0} \sim \bar{N}^{1/2}$ , and the robustness bounds are similar for different decays,  $l_{\text{max}1} \sim l_{\text{max}2} \sim \bar{N}^{1/4}$ . For  $\alpha \rightarrow \infty$ ,  $\bar{r}_m = 1$ , we recover the familiar He II healing length  $\bar{\xi} \sim (NU_0)^{-1/2}$ , with energies  $\bar{\mathcal{E}}_l \sim \bar{N} + l^2$ , and barriers  $\bar{\mathcal{E}}_{B0} \sim \bar{N}$ ,  $\bar{\mathcal{E}}_{B1} \sim \bar{N}^{1/2}$ ,  $\bar{\mathcal{E}}_{B2} \sim O(1)$ . Narrow-ring square-well containers [17] would suppress vortex loops and make phase-slips [18,24] the lowest decay thresholds. By contrast, two-dimensional harmonic traps have several (high) robustness thresholds of the same order of magnitude.

Experimental preparation of these vortex states could be through stirring normal states by a laser ‘‘paddle-wheel’’ [1] and cooling below transition; or by rotating the trap [25] with  $\Omega > \Omega_{cl}$ , below  $T_c$ ; or by coherent transfer of angular momentum from laser beams using Raman transitions [26]. Experimental detection might be through the  $l \neq 0$  density profiles, or the Sagnac effect [18,27]. An investigation of other trap geometries [28], and of attractive atoms,  $U_0 < 0$  [29], might be of interest.

In conclusion, we find that macroscopic angular-momentum states of a weakly interacting  $N$ -atoms BEC, can exist in a toroidal trap. The self-interaction creates high metastability barriers  $\sim N^{1/4}$  against various decay channels, leading to sustainable large- $l$  vortex states, that are insensitive to small toroidal hole displacements. The centrifugal force depresses the peak local density, providing a detectable signature of BEC rotation. We recover these quasi-2D results, as well as a square-well container limit, from a more general  $d$ -dimensional, anharmonic-trap scaling analysis. The observation of these rotational states would be clear evidence for the macroscopic phase coherence and superfluidity of trapped Bose-Einstein condensates.

## References

- [1] ANDERSON M. H., MATTHEWS M. R., WIEMAN C. E. and CORNELL E. A., *Science*, **269** (1995) 198; DAVIS K. B., MEWES M.-O., ANDREWS M. R., VAN DRUTEN N. J., DURFEE D. S., KURN D. M. and KETTERLE W., *Phys. Rev. Lett.*, **75** (1995) 3969; BRADLEY C. C., SACKETT C. A., TOLLETT J. J. and HULET R. G., *Phys. Rev. Lett.*, **75** (1995) 1687.
- [2] ANDREWS M. R. *et al.*, *Science*, **275** (1997) 637.
- [3] EDWARDS M. and BURNETT K., *Phys. Rev. A*, **51** (1995) 1382; RUPRECHT P. A. *et al.*, *Phys. Rev. A*, **51** (1995) 4704.
- [4] BAYM G. and PETHICK C. J., *Phys. Rev. Lett.*, **76** (1996) 6.
- [5] GRIFFIN A., *Phys. Rev. A*, **53** (1996) 9341.
- [6] JAVANAINEN J., *Phys. Rev. Lett.*, **57** (1986) 3164.
- [7] SMERZI A., FANTONI S., GIOVANNAZZI S. and SHENOY S. R., *Phys. Rev. Lett.*, **79** (1997) 4950.
- [8] RAGHAVAN S., SMERZI A., FANTONI S. and SHENOY S. R., *Phys. Rev. A*, **59** (1999) 620.
- [9] ZAPATA I., SOLS F. and LEGGETT A., *Phys. Rev. A*, **57** (1998) R28.
- [10] DODD R. J., BURNETT K., EDWARDS M. and CLARK C. W., *Phys. Rev. A*, **56** (1997) 586.
- [11] DALFOVO F. and STRINGARI S., *Phys. Rev. A*, **53** (1996) 2477; DALFOVO F. *et al.*, *Phys. Rev. A*, **56** (1997) 3840.
- [12] ROKHSAR D. S., *Phys. Rev. Lett.*, **79** (1997) 1261.
- [13] WILLIAMS G. A. and PACKARD R. E., *Phys. Rev. Lett.*, **32** (1974) 587; ESSMANN U. and TRÄUBLE H., *Phys. Lett. A*, **24** (1967) 526.
- [14] TILLEY D. R. and TILLEY J., *Superfluidity and Superconductivity*, 3rd edition (Adam Hilger, Bristol) 1990.
- [15] LITTLE W. A. and PARKS R. D., *Phys. Rev. Lett.*, **9** (1962) 9.
- [16] FETTER A. L., *Phys. Rev.*, **138** (1965) A429, A709.
- [17] a) BLOCH F., *Phys. Rev. A*, **7** (1973) 2187; PUTTERMAN S. J., KAC M. and UHLENBECK G. E., *Phys. Rev. Lett.*, **29** (1972) 546; b) PUTTERMAN S. J., *Superfluid Hydrodynamics* (North-Holland, Amsterdam) 1974, Chapt. 8.
- [18] ROKHSAR D. S., cond-mat / 9709212; MUELLER E. J., GOLDBART P. M. and LYANDA-GELLER Y., *Phys. Rev. A*, **57** (1998) R1508.
- [19] JACKSON B., MCCANN J. F. and ADAMS C. S., *Phys. Rev. Lett.*, **80** (1998) 3903.
- [20] ANDREWS M. R. *et al.*, *Phys. Rev. Lett.*, **79** (1997) 553.
- [21] Such repulsion also arises in considerations of two-species condensates. See, *e.g.*, PU H. and BIGELOW N., *Phys. Rev. Lett.*, **80** (1998) 1130, 1134.
- [22] See, *e.g.* TINKHAM M., *Introduction to Superconductivity*, 2nd edition, (McGraw-Hill, New York) 1996, p. 154.
- [23] JIN D. S. *et al.*, *Phys. Rev. Lett.*, **77** (1996) 420; YOU L. *et al.*, *Phys. Rev. A*, **55** (1997) R1581; SMERZI A. and FANTONI S., *Phys. Rev. Lett.*, **78** (1997) 3589.
- [24] ZHANG X. and PRICE J. C., *Phys. Rev. B*, **55** (1997) 3128.
- [25] MARZLIN K.-P. and ZHANG W., cond-mat/9711084.
- [26] DUM R. *et al.*, *Phys. Rev. Lett.*, **80** (1998) 2972; BOLDA E. L. and WALLS D. F., cond-mat / 9708189.
- [27] POST E. J., *Rev. Mod. Phys.*, **39** (1967) 475.
- [28] Another interesting setup is a double-toroidal trap, with  $N_1 = N, l_1 = 1 (N_2 = N, l_2 = 0)$  for toroid labelled 1(2). If the toroids are initially separated by a blocking laser sheet, its removal could result in "macroscopic quantum coherence", as discussed for quantized flux states in superconductor rings by LEGGETT A. J. *et al.*, *Rev. Mod. Phys.*, **59** (1987) 1.
- [29] WILKIN N. K., GUNN J. M. F. and SMITH R. A., *Phys. Rev. Lett.*, **80** (1998) 2265.